Experimental Demonstration of Static Shape Control

Daniel Eldred* and David Schaechter†
Jet Propulsion Laboratory, California Institute of Technology, Pasadena, California

The development of large, flexible space structures has carried with it the requirement for precision shape control—for example, maintaining the paraboloid shape of a communications antenna against the effects of thermal deformation and construction errors. Mathematically, the problem can be stated as follows: given a set of discrete sensors and actuators, select the control law which produces the "best" (in an rms sense) continuous shape as compared to some desired shape. The solution to the static shape control problem has been developed previously. This paper describes the results of a microprocessor-controlled implementation of static shape control using a flexible beam experiment.

Introduction

WITH the introduction of the Space Shuttle, larger and much more complex spacecraft (perhaps a better term is space structures) will be deployed into space. These missions will include large antennas for communication, astronomy, and radiometry; large platforms for multiple experiments; solar arrays; and perhaps even large sails for propulsion. Some of the features that these missions have in common include: 1) the structures may be accurately represented by continuum models, 2) static shape control of the continuous structures is required, and 3) distributed sensing and actuation will perform the shape control.

The mathematical theory of the optimal control of the shape of a continuous structure using a finite number of sensors and actuators has been developed[1] and yields an analytical solution. Using a Green's function approach, the continuous nature of the structure, the boundary conditions, and the discrete nature of the sensors and actuators are all handled together naturally. The existence of an analytical solution lays to rest any question about the effects of using a truncated model for control system design; however, from a practical standpoint, the actual computations are performed numerically, using a finite-element model of the structure.

The theory is made complete with experimental verification. To this end, a test facility has been constructed to demonstrate and verify various control functions associated with the static and dynamic control of large flexible space structures. In particular, this paper presents the results of a static shape control implementation on a flexible beam facility.

Derivation of the Optimal Control

Following Ref. 1, assume that the static equilibrium of an elastic, continuous structure, defined over some region Ω and subject to an applied force f, is given in terms of the linear differential operator L,

$$Ly=f \tag{1}$$

where $y(x)$ is the deflection of the structure at each point $x\in\Omega$. Furthermore, assume that boundary conditions are applied to y on the boundary Γ of Ω, such that

$$By(\Gamma)=0 \tag{2}$$

The optimal control problem consists of finding the control f which minimizes the following quadratic performance index

$$J=\frac{1}{2}\int_\Omega q(y-y_d)^2\,dx \tag{3}$$

subject to the constraints of Eqs. (1) and (2). Here, $y_d(x)$ is the desired shape. $q(x)$ is a weighting function which reflects the variable cost of shape error over Ω and should be positive for Eq. (3) to be meaningful.

The deflection which satisfies Eqs. (1) and (2) can be written in terms of the applied force $f(x)$, using the Green's function $g(x,\xi)$ for the operator (L,B). In this case,

$$y(x)=\int_\Omega g(x,\xi)f(\xi)\,d\xi \tag{4}$$

and, in the case of a finite number m of discrete concentated forces $F(x_i)$,

$$y(x)=\sum_{i=1}^{m} g(x,x_i)F(x_i) \tag{5}$$

Substituting Eq. (5) into Eq. (3) yields,

$$J=\frac{1}{2}\int_\Omega q(x)\left[\sum_{i=1}^{m} g(x,x_i)F(x_i)-y_d(x)\right]^2 dx \tag{6}$$

$$=\tfrac{1}{2}(F^TAF-2BF+C) \tag{7}$$

where

$$F=[F(x_1)F(x_2)\ldots F(x_m)]^T \tag{8}$$

$$A_{ij}=\int_\Omega g(x,x_i)g(x,x_j)q(x)\,dx \tag{9}$$

$$B_i=\int_\Omega g(x,x_i)y_d(x)q(x)\,dx \tag{10}$$

$$C=\int_\Omega y_d^2(x)q(x)\,dx \tag{11}$$

Here, A is a $m\times m$ matrix, F and B are m-dimensional vectors, and C is a scalar.

The necessary condition for F to minimize J is that $\delta J(F)=0$ for an arbitrary variation δF. Carrying out the variation, the following result obtains,

$$\delta J=\delta F^T(AF-B)=0 \tag{12}$$

Presented as Paper 81-1755 at the AIAA Guidance and Control Conference, Albuquerque, N. Mex., Aug. 19-21, 1981; submitted Nov. 16, 1981; revision received Jan. 6, 1983. This paper is declared a work of the U.S. Government and therefore is in the public domain.

*Engineer.
†Member Technical Staff.

Thus the optimal control F^* is given by

$$F^* = A^{-1}B \tag{13}$$

It is interesting to note that the absence of control weighting in Eq. (3) does not result in an unbounded control, since the convexity of the cost functional in F guarantees existence of a minimal solution. Strictly speaking, from a mathematical point of view, A^{-1} is not guaranteed to exist; in that case, the pseudoinverse can be used. A singular matrix A would result from the Green's functions $g(x,x_i)$, $i=1,\ldots,m$ being linearly dependent; this would be the case if actuators were placed at a structural node $[g(x,x_i)=0]$ or were redundant $[g(x,x_i)=g(x,x_j)]$. In practice, A is invertible (but frequently poorly conditioned) if the actuator locations are sensibly chosen.

Derivation of the Optimal Estimate

The estimation problem consists of finding the most likely shape of the structure, given a set of noisy measurements and perturbing forces which may be due to external influences or uncertainties in the control outputs. Considering the latter case, the measurement and control processes can be modeled as

$$Z = Y + V \tag{14}$$

$$F = U + W \tag{15}$$

Here, Z_i is the measurement at position $x=x_i$, Y_i the corresponding actual displacement, and V_i the measurement error. Similarly, F_i is the actual control output at $x=x_i$, U the commanded control, and W_i the process noise.

With covariance matrices Q and R defined by

$$Q = E(VV^T) \tag{16}$$

$$R = E(WW^T) \tag{17}$$

the quadratic cost functional for shape estimation becomes,

$$J = \tfrac{1}{2}(Z-Y)^T Q^{-1}(Z-Y) + \tfrac{1}{2}(F-U)^T R^{-1}(F-U) \tag{18}$$

subject to the constraint of Eq. (5), which can be rewritten as

$$Y = GF \tag{19}$$

G is the matrix whose coefficients,

$$G_{ij} = g(x_i,x_j) \tag{20}$$

give the Green's function or influence coefficients relating forces and corresponding displacements.

Adjoining Eq. (19) to Eq. (18) and using the method of Lagrangian multipliers, the cost functional without constraints becomes

$$J = \tfrac{1}{2}(Z-Y)^T Q^{-1}(Z-Y) + \tfrac{1}{2}(F-U)^T R^{-1}(F-U) + \lambda^T(Y-GF) \tag{21}$$

Minimization of Eq. (21) is straightforward and yields the optimal position estimate $\hat{y}(x)$,

$$\hat{y}(x) = \sum_i g(x,x_i)\hat{F}_i \tag{22}$$

where

$$\hat{F} = U + (R^{-1} + G^T Q^{-1} G)^{-1} G^T Q^{-1}(Z - GU) \tag{23}$$

The optimal force estimate $\hat{F}$ is of the form

$$\hat{F} = \Phi U + \Psi Z \tag{24}$$

where Φ and Ψ are constant matrices. Equation (24) is useful for the implementation of static shape control with feedback, as discussed below.

Finite-Element Models

The Green's function $g(x,\xi)$ is required for derivation of the optimal control [Eq. (13)] and the optimal estimate [Eq. (22)]. Unfortunately, an analytic solution is rarely possible, except in the case of a structure that has a particularly simple configuration. In practice, one deals with the finite-element model of the structure instead of a differential equation model, using more elements if more accuracy is desired.

The finite-element method, based on Raleigh-Ritz minimization, yields a discretized model with displacements and/or slopes at nodal points specified as coordinates or degrees of freedom. The displacement between two nodal points is given by an interpolation function (which depends on the nodal coordinates). From this and the partial differential equation for the structure, expressions for the kinetic and potential energies in terms of the nodal coordinates can be derived, which in turn define mass and stiffness matrices for a given finite element. The corresponding overall mass and stiffness matrices for the structure can be obtained as an assemblage of elemental matrices.

The inverse of the (overall) stiffness matrix, the compliance matrix, gives influence coefficients for the structure. That is, the $(i,j)^{th}$ component of the compliance matrix gives the displacement at position x_i due to a unit force applied at x_j. But this is precisely the definition of the Green's function evaluated at these two points. Summarizing, the Green's function can be evaluated at discrete, nodal points by obtaining and inverting the finite-element stiffness matrix. The required integrals in Eqs. (9) and (10) can then be evaluated using Simpson's rule or some similar numerical integration scheme.

The only approximation in the finite-element method lies in the choice of interpolation functions. For dynamic analysis, it is impossible to know a priori what the correct interpolation functions are because they are time varying; but for the static case, the exact interpolation function satisfies the time invariant differential equation subject to the boundary conditions imposed by the nodal coordinates. If exact interpolation functions are used, the resulting stiffness matrix is exact. Cubic splines are generally used for simplicity; but, even if an analytical solution to the differential equation is not known, a series solution can be used to approximate the exact interpolation function for an element if precise determination of Green's functions is required.

An alternative approach toward evaluating Green's functions is to express them as eigenvector expansions.[1] This approach requires a detailed modal model of the system (obtained from the finite-element model) and is not used here.

The Flexible Beam Facility

The flexible beam facility was constructed to demonstrate and verify various facets of control technology for large, flexible structures, including active shape control and active dynamic control.

The experiment consists of a 12½ ft. × 6 in. × 1/32 in. sheet metal beam which hangs from a supporting tower (see Fig. 1). Four sensor/actuator mounting brackets are positioned along the length of the tower (Fig. 2). Either a sensor or an actuator, or both, can be attached to a mounting bracket. Four eddy current sensors are used to provide the position at various points along the beam with an accuracy of about 3/1000 in. Stainless steel was chosen as the beam material so as to avoid any unwanted magnetic interaction with the sensors, which

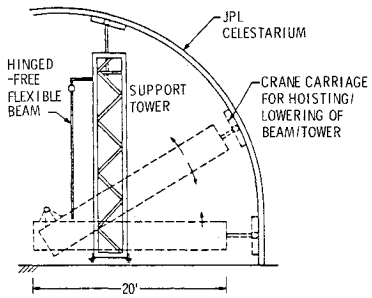

Fig. 1 Beam support structure.

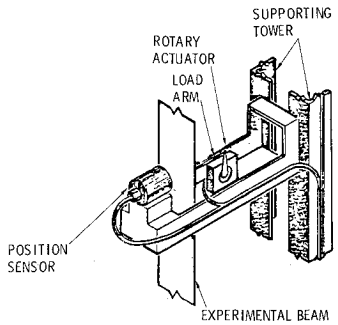

Fig. 2 Sensor/actuator mounting bracket.

are held in place with Lucite clamps. Three brushless dc motors are used for actuation and can be attached to the beam at 6 in. intervals via specially made linkages.

A 6502-based microprocessor is used to close the control loop by sampling the sensors and computing the correct commands to be sent to the actuators. The microcomputer features an advanced monitor, an editor/assembler, and BASIC, as well as the necessary analog/digital and digital/analog converters required for sensing and control output. Commonly used machine-language subroutines are stored in erasable, programmable read-only memories (EPROM) and programs and data are stored on cassette tape, using an inexpensive audio cassette recorder. An effort has been made to create a "friendly" interactive system; to this end, all programming is done in a combination of languages: BASIC to handle the user interface and to perform various calculations and initializations, and 6502 machine language for the time-critical tasks.

The relevant beam parameters are summarized in Table 1. The reader is referred to Ref. 2 for a more detailed description of the experiment, particularly for the dynamic control applications. It should be mentioned that the values in Table 1 are based on experimental results rather than tabulated values; for example, the stiffness of the beam EI was evaluated from an experiment that directly yielded the force-deflection relationship of the beam.[3]

Analysis of the Beam

The Green's function for the beam is required for calculation of the optimal control [Eq. (13)] and the optimal estimate [Eq. (23)]. An analytical approach to the solution of the Green's function requires solving the partial differential equation for the static shape $y(x)$,

$$\frac{\partial^2}{\partial x^2}\left(EI\frac{\partial^2 y}{\partial x^2}\right)-\frac{\partial}{\partial x}\left(\rho g(\ell-x)\frac{\partial y}{\partial x}\right)=f(x) \tag{25}$$

with boundary conditions,

$$y(0)=\frac{\partial^2 y}{\partial x^2}(0)=0 \qquad \frac{\partial^2 y}{\partial x^2}(\ell)=\frac{\partial^3 y}{\partial x^3}(\ell)=0 \tag{26}$$

The following change of variables,

$$z=(\rho y/EI)^{1/5}(\ell-x) \tag{27}$$

considerably simplifies the homogeneous equation,

$$\frac{\partial^4 y}{\partial z^4}-\frac{\partial}{\partial z}\left(z\frac{\partial y}{\partial z}\right)=0 \tag{28}$$

whose solution can be expanded about $z=z_0$ in a Taylor series,

$$y(z)=\alpha_0\phi_0(z)+\alpha_1\phi_1(z)+\alpha_2\phi_2(z)+\alpha_3\phi_3(z) \tag{29}$$

where

$$\begin{aligned}
\phi_0(z)&=1\\
\phi_1(z)&=(z-z_0)+\frac{(z-z_0)^4}{4!}+\ldots\\
\phi_2(z)&=\frac{(z-z_0)^2}{2!}+z_0\frac{(z-z_0)^4}{4!}+\ldots\\
\phi_3(z)&=\frac{(z-z_0)^3}{3!}+z_0\frac{(z-z_0)^5}{5!}+\ldots
\end{aligned} \tag{30}$$

The recursion relation relating coefficients of $(z-z_0)^n$ is given by

$$a_{n+3}=\frac{na_n}{(n+1)(n+2)(n+3)}+\frac{z_0 a_{n+1}}{(n+2)(n+3)} \qquad n=1,2,3,\ldots \tag{31}$$

The series solution [Eq. (29)] to the homogeneous equation was used as the interpolation function for derivation of the finite-element stiffness matrix. The resulting Green's function matrix, obtained by inversion of the stiffness matrix, gives the influence coefficients at nodal points that are essentially exact. In practice, a 20 element model, which specifies as coordinates the displacement and slope at each nodal point, has proved to be satisfactory for both static and dynamic analysis.

Verification of the finite-element model was accomplished by computing the eigenvalues of the dynamic system and

Table 1 Beam parameters

Variable	Value	Description
ℓ	149.875 in.	Beam length
ρ	0.6444 lb/ft	Linear density
EI	424.352 lb-in.^{2}	Beam stiffness

Table 2 Normal mode frequencies, Hz

n	10 divisions	20 divisions	Experimental
0	0.308	0.308	~0.34
1	0.755	0.755	0.75
2	1.38	1.38	1.37
3	2.21	2.21	2.15
4	3.25	3.24	3.16
5	4.51	4.47	4.38

comparing them with the experimentally determined normal mode frequencies. The results are summarized in Table 2.

The coefficients A_{ij} and B_i in Eq. (13) were determined from a straightforward application of Simpson's rule for numerical integration.

Demonstration of Shape Control

Two desired shapes $y_d(x)$ were chosen for demonstration of shape control,

$$\text{Shape I:} \quad y_d(x) = \tfrac{1}{2}\left(\frac{2x}{\ell} - \frac{x^2}{\ell^2}\right) \text{ in.} \tag{32}$$

$$\text{Shape II:} \quad y_d(v) = \tfrac{1}{2}\left(\frac{4x}{\ell} - \frac{4x^2}{\ell^2}\right) \text{ in.} \tag{33}$$

Shape I consists of a parabola with its vertex located at the bottom end of the beam and shape II is a parabola which is symmetric about the middle of the beam.

The optimal control F^* is given by Eq. (13),

$$F^* = A^{-1}B$$

For the flexible beam, the analysis outlined above yields

$$A = \begin{bmatrix} 625 & 380 & 241 \\ 380 & 252 & 167 \\ 241 & 167 & 115 \end{bmatrix} \text{ in.}\cdot\text{s}^4/\text{slug}^2 \tag{34}$$

$$B_{\text{I}} = \begin{bmatrix} 101.8 \\ 69.9 \\ 47.9 \end{bmatrix} \text{ in.}^2\cdot\text{s}^2/\text{slug} \tag{35}$$

and

$$B_{\text{II}} = \begin{bmatrix} 67.8 \\ 55.1 \\ 42.4 \end{bmatrix} \text{ in.}^2\cdot\text{s}/\text{slug} \tag{36}$$

B_{I} and B_{II} refer to the B vectors for shapes I and II. The corresponding optimal controls are given by

$$F_I^* = \begin{bmatrix} 0.0213 \\ -0.0267 \\ 0.4093 \end{bmatrix} \text{slug}\cdot\text{in.}/\text{s}^2 \tag{37}$$

$$F_{II}^* = \begin{bmatrix} -0.0919 \\ -0.3326 \\ 1.0413 \end{bmatrix} \text{slug}\cdot\text{in.}/\text{s}^2 \tag{38}$$

With the covariances given by

$$Q = 6.25\times10^{-6} \text{ in.}^2 \tag{39}$$

$$R = 2.2\times10^{-4} \text{ in.}^2 \text{ slug}^2/\text{s}^4 \tag{40}$$

the optimal estimate using all four sensors and three actuators

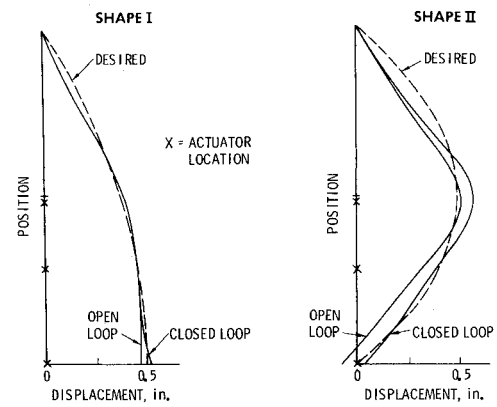

Fig. 3 Open and closed loop shape control.

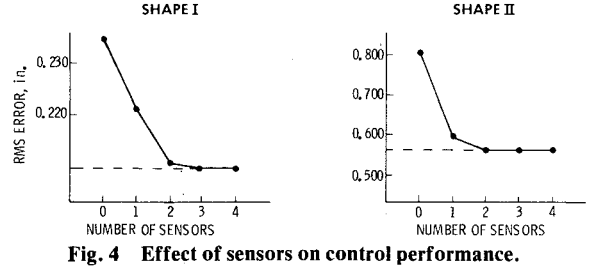

Fig. 4 Effect of sensors on control performance.

is given by

$$\hat{y}(x) = \sum_{i=1}^{3} g(x,x_i)\hat{F}_i \tag{41}$$

where $\hat{F}$ is determined from

$$\hat{F} = \begin{bmatrix} 0.368 & -0.413 & -0.004 & 0.038 \\ -0.420 & 1.66 & -0.898 & -0.603 \\ 0.021 & -1.14 & 1.610 & 0.907 \end{bmatrix} \begin{bmatrix} Z_1 \\ Z_2 \\ Z_3 \\ Z_4 \end{bmatrix} + \begin{bmatrix} 0.012 & -0.042 & 0.032 \\ -0.042 & 0.218 & -0.219 \\ 0.033 & -0.219 & 0.252 \end{bmatrix} \begin{bmatrix} U_1 \\ U_2 \\ U_3 \end{bmatrix} \tag{42}$$

The displacements resulting from shape control are shown in Fig. 3 for the two chosen desired shape functions. Assuming zero initial displacement of the beam, the control forces given by Eqs. (37) and (38) result in the shapes labeled "open loop." The relatively large biases are primarily due to hysteresis torque in the actuators. Recall that the analysis assumed that the process noise was Gaussian with zero mean. For an ensemble of shape control experiments, this might be the case, but for one given shape control experiment, the hysteresis torque comes in as a constant bias. Clearly an iterative control scheme is needed.

The shapes labeled "closed loop" in Fig. 3 are the result of using feedback to further improve the controlled shape. One iteration of the control loop consists of the following steps: the sensors are sampled, an estimate of the actuator forces is obtained using Eq. (42), and finally new control outputs are obtained based on the difference between the optimal outputs and the estimate of the actual outputs. The feedback loop is

completed by repeatedly iterating this control loop, allowing any vibrations in the beam to die out between successive applications of control. The process is repeated until no further change in the shape is observed (usually two or three iterations).

The feedback scheme depends on using the sensor measurements for estimation prior to each control force computation. It is natural to ask the question of how many sensors are required to do a "good" control job. Therefore, the rms error in the shape (i.e., the difference between the desired and actual shapes) is shown in Fig. 4 as a function of the number of sensors used in the control loop. These results show that the addition of more than one or two sensors to the control loop does little to improve performance. It can be reasonably asserted that few sensors are required if the system model is initially "good," and that more are required for feedback if modeling errors exist.

Conclusions

This paper documents the implementation of static shape control on a flexible beam experiment. Demonstration of the static shape control required the integration of many diverse activities, including development of shape control algorithms, adaptation of the algorithms for use with finite-element models, construction of the flexible beam, characterization and calibration of the facility, development of the finite-element model for the beam, and the development of computer hardware and software.

It was shown that open-loop control yields poor results as compared to feedback control. Furthermore, performance is not significantly improved by the use of more than two sensors in the control loop. The latter property can be of great importance to the control analyst who must choose how many sensors to use.

Acknowledgments

The research described in this paper was performed by the Jet Propulsion Laboratory, California Institute of Technology, under contract with the National Aeronautics and Space Administration.

References

[1]Weeks, C. J., "Shape Determination and Control for Large Space Structures," Jet Propulsion Laboratory, Rept. 81-71, Oct. 1981.

[2]Schaechter, D.B., "Hardware Demonstration of Flexible Beam Control," *Journal of Guidance and Control,* Vol. 5, Jan. 1982, pp. 48-53.

[3]Eldred, D.B., "Finite Element Model for the LSST Beam," Jet Propulsion Laboratory, Rept. EM 347-101, 1981.

From the AIAA Progress in Astronautics and Aeronautics Series . . .

COMMUNICATIONS SATELLITE SYSTEMS—v. 32

Edited by P. L. Bargellini, Comsat Laboratories
A companion to Communications Satellite Technology, volume 33 in the series.

The twenty papers in this volume deal with international applications, advanced concepts, and special topics, covering the lessons and technical advancements resulting from the Intelsat II program of eight launches in the years 1966-1970. Includes Intelsat V system concepts and technology, with implications for multiple access, power generation and storage, and propellant utilization. It also includes proposals for U.S.-European cooperation in satellite applications programs of the Intelsat system.

Advanced concepts discussed include the coming generation of flexible communications satellites, with variations in switching, applications, and payloads; a dual-beam antenna for broadcast band service; high-powered, three-axis stabilized, position-keeping satellites; commercial communications with ships or aircraft via stationary satellites; multiple beam phased antennas; complex ground stations and relatively straightforward equipment on the satellite; and research in manned orbital laboratories.

Special topics include two-way telephonic communication via satellite, various education and information transfer systems, and a centralized radio-frequency data base for satellite communication system design.

480 pp., 6 x 9, illus. $14.00 Mem. $20.00 List

TO ORDER WRITE: Publications Dept., AIAA, 1290 Avenue of the Americas, New York, N. Y. 10019